Event simulations in a transport model for intermediate energy heavy ion collisions: Applications to multiplicity distributions

S. Mallik,[1] S. Das Gupta,[2] and G. Chaudhuri[1]
[1]*Theoretical Physics Division, Variable Energy Cyclotron Centre, 1/AF Bidhan Nagar, Kolkata 700064, India*
[2]*Physics Department, McGill University, Montréal, Canada H3A 2T8*
(Received 24 November 2014; revised manuscript received 19 February 2015; published 26 March 2015)

We perform transport model calculations for central collisions of mass 120 on mass 120 at laboratory beam energy in the range 20 MeV/nucleon to 200 MeV/nucleon. A simplified yet accurate method allows calculation of fluctuations in systems much larger than what was considered feasible in a well-known and already existing model. The calculations produce clusters. The distribution of clusters is remarkably similar to that obtained in equilibrium statistical model.

DOI: 10.1103/PhysRevC.91.034616 PACS number(s): 25.70.Mn, 25.70.Pq, 24.10.Lx, 24.10.Nz

I. INTRODUCTION

There is an enormous amount of experimental and theoretical work on multifragmentation in heavy ion collisions at intermediate energy. There are two classes of theoretical models: (a) dynamical and (b) statistical where one assumes that because of two-body collisions the colliding systems equilibrate and break up into many fragments according to availability of phase space. Unquestionably the most used and popular dynamical model is the Boltzmann-Uehling-Uhlenbeck (BUU) model (also called by various other names). Here we restrict ourselves to BUU [1]. In the original formulation, the BUU model gave an account of one-body properties [2] and thus was not suitable to describe multifragmentation. Later it was extended to include fluctuations which made it suitable for event-by-event simulation [3]. This is the focus of our attention. In the past event-by-event simulation in this model was limited to about mass number 30 on 30. The problem was a practical one, namely, it required a large computing effort. We show that with a slight reformulation without changing any physics or numerical accuracy we can very significantly reduce the execution time and we can handle much larger systems. Computation becomes as short as an ordinary BUU calculation. It is instructive to do large systems (finite number effects often hide important bulk effects) and more importantly, the fragmentation must be investigated over an energy range to unravel many interesting effects. The objective of doing examples is to demonstrate that many revealing features are seen. These also allow us to relate with other models.

There are many models for multifragmentation. There are some which can be labeled as "quantum molecular dynamics" type [4,5]. These are different in spirit to the model used here. Closer in spirit yet quite distinct are some studies based on a Langevin model [6–10], where we have mentioned only a few. We will have occasion to refer very briefly to only a small number of these. The literature in the Langevin approach is huge.

II. THE PRESCRIPTION

The basic features of our transport model calculation are contained in the BUU model as developed in [1] and [3] but some modifications were made. For brevity we will almost entirely skip the physical motivations and details for the models of Refs. [1,3] as they are not only adequately discussed in the original papers but also elsewhere [8,9] where some different models are also introduced. The modifications we make to Refs. [1,3] are discussed fully.

The start of our consideration is the cascade model [11]. Here each nucleus is considered as a collection of point nucleons whose positions are assigned by Monte Carlo sampling. The projectile nucleus A approaches the target B with a beam velocity and two-body collisions between the nucleons take place. When these finish we have one event. We only consider B the same as A and central collisions. It is convenient to run several events simultaneously. Let us label the number of runs by $\tilde{N}$. In cascade the different runs do not communicate with each other. Thus nucleus 1 hits nucleus $1'$, nucleus 2 hits nucleus $2', \ldots,$ nucleus $\tilde{N}$ hits nucleus $\tilde{N}'$. In BUU we introduce the communication between runs. What we were calling nucleons we now call test particles (abbreviated from now on as tp). The density $\rho(\vec{r})$ is given by $n/(\delta r)^3\tilde{N}$ where n is the number of tp's in a small volume $(\delta r)^3$. As far as collisions go, in usual applications of BUU one still segregates different runs. By segregating the collisions one is able to use σ_{nn}, the nucleon-nucleon cross section, and reduce computation. If we considered collisions between all tp's, the collision cross sections would have to be reduced. In between collisions tp's move in a mean field (Vlasov propagation). Applications of BUU as summarized above have met much success in explaining average properties such as average collective flows, etc.

To explain multifragmentation, multiplicity n_a as a function of a, where a is the mass number of the composite, one needs an event-by-event computation in the transport model. Bauer *et al.* made the following prescription [3]. Now all tp's are allowed to collide with one another with a cross section of $\sigma_{nn}/\tilde{N}$. Collisions are further suppressed by a factor $\tilde{N}$ but when two tp's collide not only those two but $2(\tilde{N}-1)$ tp's contiguous in phase space change momenta also. Physically it represents two actual particles colliding. When collisions cease we have one event. A second event needs a new Monte Carlo of tp's and then the evolution in time.

The prescription we use here is the following. This is the middle ground between Refs. [1] and [3]. As in Ref. [1] for nucleon-nucleon collisions we consider 1 on $1'$(event1), 2 on

$2'$(event2), etc., with cross section σ_{nn}. For event 1 we will consider nn collisions only between 1 and $1'$. The collision is checked for Pauli blocking as in Ref. [1]. If a collision between i and j in event 1 is allowed we follow Ref. [3] and pick $\tilde{N}-1$ tp's from all the tp's closest to i and give them the same momentum change $\Delta\vec{p}$ as ascribed to i. Similarly we pick $\tilde{N}-1$ tp's closest to j and ascribe them the momentum change $-\Delta\vec{p}$, the same as suffered by j. We will return to more details about this later. As a function of time this is continued till event 1 is over. For event 2 we return to time $t=0$, the original situation (or a new Monte Carlo sampling for the original nuclei), follow the above procedure but consider nn collisions only between 2 and $2'$. This can be repeated for as many events as one needs to build up enough statistics. The advantage of this over that used in Ref. [3] is that here, for one event, nn collisions need to be considered between (N_A+N_B) nucleons (N_A = number of nucleons in A, N_B = number of nucleons in B) whereas in the method of Ref. [3], collisions need to be checked between $(N_A+N_B)\times\tilde{N}$ tp's. Hence, in our calculation, the total number of combinations for a two-body collision is reduced by a factor of $1/\tilde{N}^2$. Since typically $\tilde{N}$ is of the order of 100 this is a huge saving in computation and has allowed us to treat mass as large as 120 on 120 over a substantial energy range. It is expected that the model used in Ref. [3] and the one used here will give similar results. The number of collisions for one event should be about the same in both prescriptions. The characteristics of scattering are the same. The objects that collide in our calculation arise from a coarse grain representation of the initial phase space population of two nuclei. In Ref. [3] a fine grain representation is used. But since many events are generated any difference should disappear. The Vlasov propagation is the same. For mass 40 on 40 we compare our results with those using the method of Ref. [3] (Fig. 1). The agreement between the two calculations for multiplicities is remarkable. We regard our method as a very convenient shortcut to the numerical modeling of Ref. [3]. The theoretical formulation in Ref. [3] is more appealing and "democratic" but numerically our method gives indistinguishable results.

One bonus of our prescription is that one sees some common ground between the BUU approach and the "quantum molecular dynamics" approach. In the latter nucleons are represented by Gaussians in phase space; the centroids have an $\vec{r}$ and a $\vec{p}$ which are originally generated by Monte Carlo calculations. These collide. This corresponds to "nucleons" colliding in our prescription. As the centroids move after collision, they drag the Gaussians along. The Gaussian wave packets in position and momentum space provide the mean-field and Pauli blocking. The Gaussians do not change their shapes or widths. These are very strong restrictions and lead to very different mean field propagation. The Vlasov propagation has much more flexibility and originates from more fundamental theory.

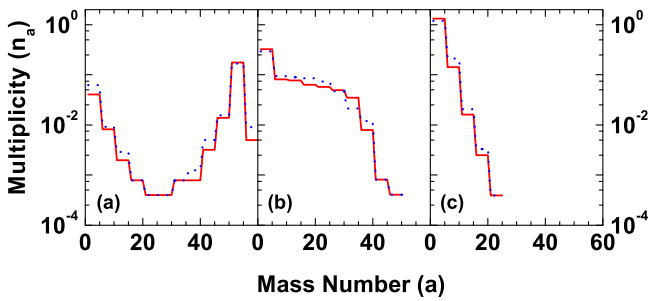

FIG. 1. (Color online) Comparison of mass distribution calculated according to the prescription of Ref. [3] (blue dotted lines) and the present work (red solid lines). The average value of 5 mass units are shown. The cases are for central collision of mass 40 on mass 40 for different beam energies (a) 25, (b) 50, and (c) 100 MeV/nucleon. 500 events were chosen at each energy.

III. SOME DETAILS OF THE SIMULATIONS

We provide some details of the calculation. For Vlasov propagation we use the lattice Hamiltonian method [12] of Lenk and Pandharipande which accurately conserves energy and momentum. The mean field Hamiltonian for Vlasov propagation is also adopted from that work. The potential energy density is

$$v(\rho(\vec{r}))=\frac{A}{2}\rho^2(\vec{r})+\frac{B}{\sigma+1}\rho^{\sigma+1}(\vec{r})+\frac{c\rho_0^{1/3}}{2}\frac{\rho(\vec{r})}{\rho_0}\nabla_r^2\left[\frac{\rho(\vec{r})}{\rho_0}\right]. \tag{1}$$

The values of the constants are $A=-2230.0\text{MeVfm}^3$, $B=2577.85$ MeV fm$^{7/2}$, $\sigma=7/6$, $\rho_0=0.16$ fm^{-3}, $c=-6.5$ MeV. The last term in the right hand side of Eq. (1) gives rise to surface energy in finite nuclei. That favors the formation of larger composites, for example, the occurrence of a nucleus of A nucleons over the formation of two nuclei of $A/2$ nucleons. Entropy works the other way.

Further details are

(1) Calculations were done in a $200\times200\times200$ fm^3 box. The configuration space was divided into 1 fm^3 boxes.

(2) For results shown here the code was run from $t=0$ fm/c to $t=200$ fm/c. Positions and momenta of tp's were updated every $\Delta t=0.3$ fm/c.

(3) For nucleon-nucleon collision we follow Appendix B. of Ref. [1].

(4) The number $\tilde{N}$ was set at 100.

(5) Once the two-body collisions are nearly over, contiguous boxes with tp's that propagate together for a long time are considered to be part of the same cluster. The contiguous boxes have at least one common surface and the nuclear density exceeds a minimum value ($d_{\min}$). Different $d_{\min}$ values as 0.002, 0.005, 0.01, 0.015, and 0.02 fm^{-3} are tried to check the sensitivity of this parameter. It is observed that the fragment multiplicity distribution is not changing very much with $d_{\min}$, therefore we use $d_{\min}=0.01$ fm^{-3} for further calculations.

IV. RESULTS

In Fig. 2 we show plots of multiplicity against mass number a for 120 on 120. Four beam energies are shown. For each energy 1000 events were taken. We show results of averages for groups of five consecutive mass numbers. The prominent feature we wish to point out is that at low

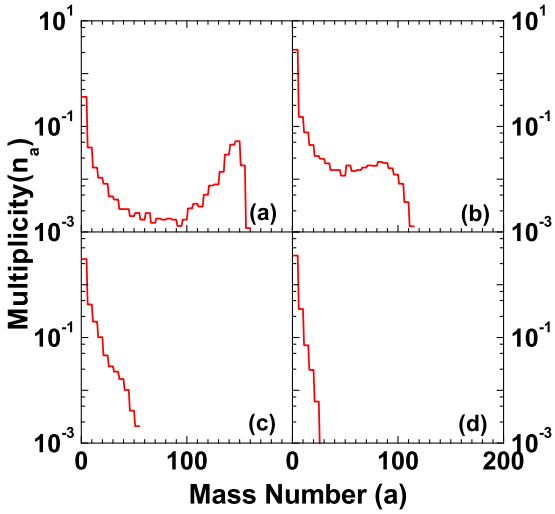

FIG. 2. (Color online) Mass distribution from BUU model calculation for $N_A = 120$ on $N_B = 120$ reaction at beam energies (a) 50 MeV/nucleon, (b) 75 MeV/nucleon, (c) 100 MeV/nucleon, and (d) 150 MeV/nucleon. The average value of 5 mass units is shown. At each energy 1000 events are chosen. Only central collisions are considered here but even at $E_p = 50$ MeV/nucleon, nucleons in the peripheral region passes through and largest fragment remaining is less than the sum of the masses of the two nuclei.

beam energy (50 MeV/nucleon) the multiplicity first falls with mass number a, reaches a minimum, then rises, reaches a maximum before disappearing. As the beam energy increases the height of the second maximum decreases. At beam energy 75 MeV/nucleon the second maximum is still there but barely. At higher energy the multiplicity is monotonically decreasing, the slope becoming steeper as the beam energy increases. This evolution of shape of the multiplicity distribution is of significance as we will emphasize soon but let us point out this evolution of shape was a long time prediction of the

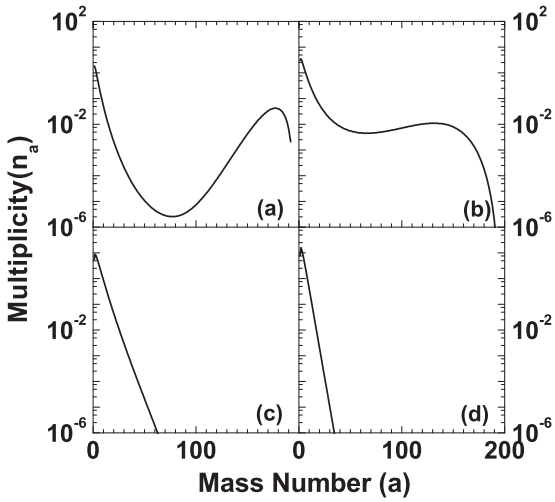

FIG. 3. Mass distribution from the canonical thermodynamical model (CTM) calculation for fragmentation of a system of mass $A_0 = 192$ at temperature (a) 6.5 MeV, (b) 7.5 MeV, (c) 10 MeV, and (d) 14 MeV.

canonical thermodynamic model (CTM) [13,14]. For transport models the natural variable is the beam energy. For CTM the natural variable is the temperature T. For illustration we have shown the multiplicity distribution for a system of 192 particles in CTM at temperatures of 6.5 MeV, 7.5 MeV, 10 MeV, and 14 MeV (Fig. 3). The calculations with BUU and CTM are so different that the similarity in the evolution of the shape in multiplicity distribution is very striking. Indeed this correspondence provides the support for assumptions of statistical model from a microscopic calculation.

To proceed further with the correspondence between the two models we need to establish a connection between E_p of BUU and temperature T of CTM. Temperature T of CTM will give an average excitation energy E^* of the multifragmenting system in its center of mass (c.m.) [14]. We can calculate the excitation energy (E^*) in the c.m. from (E_p) by direct kinematics by assuming that the projectile and the target fuse together. In that case the excitation energy is $E^* = A_p E_p/(A_p + A_t)$, where A_p and A_t are projectile and target masses, respectively. This value is too high as a measure of the excitation energy of the system which multifragments. The nucleons at the edges of the two nuclei pass through carrying a lot of energy and are not part of the multifragmenting system. These are pre-equilibrium particles. In experiments about 20% of nucleons are emitted as fast pre-equilibrium particles: see for example [15,16]. Further details can be found in Ref. [17] but this is what we do basically. We go to the cm of the two ions to do BUU and at the end discard 20% particles (these have the highest energies), and measure energy (potential plus kinetic) of the rest. To find the excitation energy we subtract Thomas-Fermi ground-state energy of the rest with the Hamiltonian of Eq. (1).

Figure 4 gives some CTM results and also makes a comparison of one CTM result with transport model result. The top left diagram is E^* vs. T in CTM for 192 particles ($A_0 = 192 = 80\%$ of 240). This approximates usual E^* vs T for first-order phase transition. There is a boiling point temperature T which remains constant as energy increases. In the example here, because we have a very finite system, the slope dE^*/dT is not infinite but high. Let us now consider lower left diagram again drawn in CTM. Here $A_{\max}$ is the average value of the largest cluster. A high value of $A_{\max}/A_0$ means liquid phase and low values means gas phase. The criteria of deciding which composites belong to the gas phase and which to the liquid phase are discussed in detail in two previous papers [18,19].

In the bottom left diagram, one sees more dramatically that in a short-temperature interval liquid has transformed into gas. The only input in our transport model is the beam energy. The common dynamical variable in both our model and CTM is E^*. Of course the E^* in CTM is an average whereas the E^* in transport model is a microcanonical E^*. In the top right corner of Fig. 4 is the plot of $A_{\max}/A_0$ as a function of E^* in CTM. The transformation from liquid to gas is more gradual, essentially spanning the energy range across which, liquid transforms totally into gas. Even for a large system, where the transformation of liquid to gas as a function of temperature is very abrupt, the transformation as a function of energy per particle will be quite smooth. The bottom right in

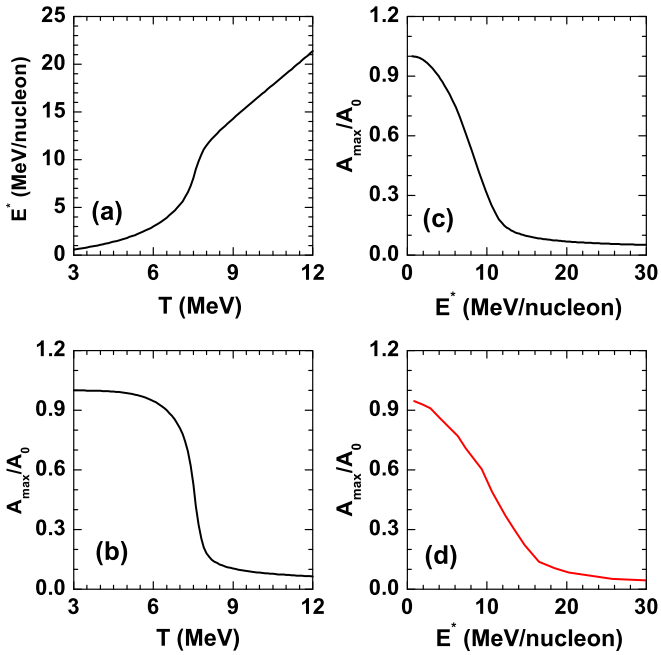

FIG. 4. (Color online) Top left curve (a) is a canonical thermodynamical model (CTM) calculation for excitation (E^*) vs. temperature (T) for $A_0 = 192$. Between 6 MeV and 7.5 MeV temperatures, E^* rises quickly. The dE^*/dT slope increases sharply with mass size A_0 and is indicative of first-order phase transition. Bottom left curve (b) is also a CTM curve showing that the size of largest cluster drops sharply between 6 MeV and 7.5 MeV. Again this is a first-order liquid gas phase transition. Top right (c) is also with CTM but $A_{\max}/A_0$ is plotted against excitation energy per nucleon instead of temperature. The change of liquid to gas is necessarily slower, the range of energy for the change is dictated by latent heat. Bottom right (d) is the calculation from transport model.

Fig. 4 is from our transport model calculation. The similarity with the CTM graph is close enough that we conclude the transport model calculation gives evidence of liquid-gas phase transition. To find closer correspondence between transport model calculations and CTM, it will be best if we can deduce at least an approximate value of temperature for each beam energy. For an interacting system this is very nontrivial. Formulas like $\frac{E^*}{A} = \frac{3T}{2}$ are obviously inappropriate. One might try to exploit the thermodynamic identity $T = (\frac{\partial E}{\partial S})_V$. This requires obtaining a value of the entropy for an interacting system. We will be working on this in future.

In concluding this section, we mention that while we have established a correspondence between transport model results and CTM results, a more natural choice would have been to compare transport model results with multiplicity distributions obtained from the microcanonical statistical multifragmentation model (SMM) [20]. These are not available to us. However for the only cases investigated we found that CTM and SMM results were quite close [21] so the correspondence we have found here between transport model results and CTM will presumably hold for SMM also. Multiplicity distributions in $^{16}O + ^{80}Br$ were done with dynamic models before. The work in Ref. [22] used molecular dynamics. The work in Ref. [23] comes closer in spirit to ours. The colliding system was small and no attempt was made to link the work with statistical models or phase transition.

V. DISCUSSION

We now look at one feature of the model that raised concerns and led to a lot of work to propose alternative methods for calculations [9,10]. This is related to dangers of crossing fermionic occupation limits in the model here (as in the model of Ref. [3]). As mentioned already, if Pauli blocking allows two tp's i and j to collide, then not only these two but also $\tilde{N}-1$ tp's closest to i and $\tilde{N}-1$ closest to j move to represent that two actual nucleons scatter. The tp's that move with i are denoted by i_s, with $s = 0$ to $\tilde{N}-1$. The square of the distance is taken to be $d_{0s}^2 = \frac{(\vec{r}_{io}-\vec{r}_{is})^2}{R^2} + \frac{(\vec{p}_{io}-\vec{p}_{is})^2}{p_F^2}$. Here R is the radius of the static nucleus of $A = 120$ and p_F the Fermi momentum.. The tp's j_s are then chosen from the rest of the tp's. Define now $\langle\vec{p}_i\rangle = \frac{\sum \vec{p}_{is}}{\tilde{N}}$, similarly $\langle\vec{p}_j\rangle$. One then considers a collision between $\langle\vec{p}_i\rangle$ and $\langle\vec{p}_j\rangle$ and obtain a $\Delta\vec{p}$ for $\langle\vec{p}_i\rangle$ and $-\Delta\vec{p}$ for $\langle\vec{p}_j\rangle$. This $\Delta\vec{p}$ is added to all $\vec{p}_{is}$ and $-\Delta\vec{p}$ to all $\vec{p}_{js}$. Since the tp's are moved without verifying Pauli blocking there may be cases where one exceeds the occupation limits for fermions.

Initially the two ions have a very compact occupation at two different corners of phase space. Collisions make a far wider region of phase space available to nucleons so this problem may not be severe. An accurate estimation of exceeding the fermionic limit of occupation at various parts of phase space is very hard to compute in our present problem but some measures are relevant.

For 120 on 120 at 100 MeV/nucleon beam energy (50 MeV/nucleon beam energy was studied also) we follow one event as a function of time. In every collision in the event, $2\tilde{N}$ tp's change momenta. To be specific, let the tp i_s move from $\vec{r}, \vec{p}_{in}$ to $\vec{r}, \vec{p}_{fi}$. We check if by moving i_s to the final phase space point $(\vec{r}, \vec{p}_{fi})$ we cross the fermionic limit. We build a six-dimensional unit cell in phase space around this final phase space point [1,24]. The volume of the unit cell Should be small so that one is investigating the phase-space occupation very near $(\vec{r}, \vec{p}_{fi})$, but it cannot be too small since Monte Carlo simulation has noise which can cloud the actual effect. In accordance with past calculations we chose a volume of unit cell in phase space where eight tp's is the maximum number allowed for fermions. If n is the number of tp's (not including i_s) already in the unit cell we define an availability factor $\tilde{f} = 1.0 - n/8$. If $\tilde{f} = 0$ we are already at the limit of fermionic occupation. If $\tilde{f}$ is negative we have crossed the quantum limit and are in the classical regime. Any positive number between 0 and 1 will accommodate additional fermion. For each collision there are 200 $\tilde{f}$'s to be calculated so for each collision we get an ave $\tilde{f}$ and that is plotted in Fig. 5. We have shown results for $t = 25$ to 125 fm/c when most of the action takes place. For reference we also plot average $\tilde{f}$ for randomly chosen 120 tp's in a static mass 120 nucleus as they move around in time. This number should ideally be 0 and not fluctuate. The deviations from zero in the static case probably largely arise due to fluctuations in Monte Carlo sampling. This degree of uncertainty must be also present in the values of $\tilde{f}$ we have plotted for collisions. In spite of these uncertainties the

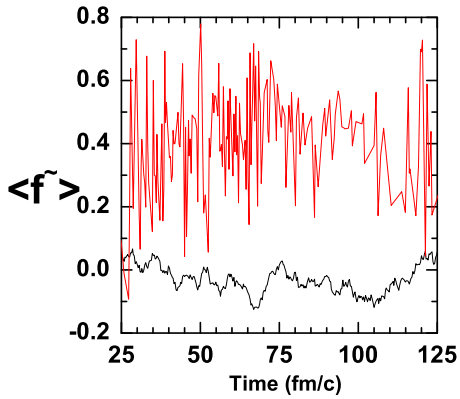

FIG. 5. (Color online) Variation of average availability factor (see text) with time (red line) for $N_A = 120$ on $N_B = 120$ reaction at beam energy 100 MeV/nucleon. The lower curve (black dotted line) is the average availability factor $\langle \tilde{f} \rangle$ at the phase space points of arbitrarily chosen 120 test particles in an isolated mass 120 nucleus as they move in time. The fluctuations from the value 0 reflects uncertainties, probably due to fluctuation in initial Monte Carlo simulations.

predominantly positive values of $\tilde{f}$ as displayed in Fig. 5 lead us to believe that the general trends we find in our calculation will hold.

If in a collision all of the 200 tp moved to locations where $\tilde{f}$ were all positive we will stay within the fermionic limits. In case there is a tp which does not satisfy this we can try to improve the situation by discarding that tp and choosing the next available tp to be part of the cloud. Complications arise because when some of the previously chosen tp's are discarded for new ones the average momentum of the clouds will change, new $\Delta\vec{p}$ will have to be used so the final resting spots obeying energy and momentum conservation will change too. An iterative procedure needs to be formulated but convergence may be slow.

Alternative methods have been proposed. The two papers which give procedural details of moving two clouds of tp's from initial positions to final positions with a stricter adherence to fermionic limits are Refs. [9,10]. Multiplicity distributions are not given so we cannot compare. Even if the multiplicity distributions turn out to be similar, higher order correlations can be very different. The present work extended the first proposed model of fluctuations in BUU to a larger system at many energies and a very interesting lesson was learned. The gross features of multiplicity distribution do resemble strongly the results from equilibrium statistical models which have proven very successful in explaining experimental data.

VI. SUMMARY

An event-by-event simulation of a transport model was made at collisions of moderately heavy ions at zero impact parameter. Multiplicity distributions were calculated. They are remarkably similar to those obtained from a equilibrium statistical model (CTM). This work therefore justifies the use of the equilibrium statistical model for data fitting. This statistical model implies first order phase transition in large nuclear systems at finite temperature. It will be of interest to quantify more precisely the correspondence of transport model result and statistical model results. That work is in progress.

ACKNOWLEDGMENTS

Part of this calculation was performed in Variable Energy Cyclotron Centre (VECC) and part at McGill University. S.D.G. thanks the director of VECC Dr. D. K. Srivastava for his strong support for the project and hospitality. He also thanks Dr. A. K. Chaudhuri for hospitality. S.M. thanks the physics department of McGill University for a very productive and pleasant stay in Montreal. This work was supported in part by Natural Sciences and Engineering Research Council (NSERC) of Canada.

[1] G. F. Bertsch and S. Das Gupta, Phys. Rep. **160**, 189 (1988).
[2] G. F. Bertsch, H. Kruse, and S. Das Gupta, Phys. Rev. C **29**, 673(R) (1984).
[3] W. Bauer, G. F. Bertsch, and S. Das Gupta, Phys. Rev. Lett. **58**, 863 (1987).
[4] J. Aichelin and H. Stocker, Phys. Lett. B **176**, 14 (1986).
[5] G. E. Beauvais, D. H. Boal, and J. C. K. Wong, Phys. Rev. C **35**, 545 (1987).
[6] S. Ayik and C. Gregoire, Nucl. Phys. A **513**, 187 (1990).
[7] J. Randrup and B. Remaud, Nucl. Phys. A **514**, 339 (1990).
[8] Ph. Chomaz, G. F. Burgio, and J. Randrup, Phys. Lett. B **254**, 340 (1991).
[9] J. Rizzo, Ph. Chomaz, and M. Colonna, Nucl. Phys. A **806**, 40 (2008).
[10] P. Napolitani and M. Colonna, Phys. Lett. B **726**, 382 (2013).
[11] J. Cugnon, T. Mizutani, and J. Vandermeulen, Nucl. Phys. A **352**, 505 (1981).
[12] R. J. Lenk and V. R. Pandharipande, Phys. Rev. C **39**, 2242 (1989).
[13] S. Das Gupta and A. Z. Mekjian, Phys. Rev. C **57**, 1361 (1998).
[14] C. B. Das, S. Das Gupta, W. G. Lynch, A. Z. Mekjian, and M. B. Tsang, Phys. Rep. **406**, 1 (2005).
[15] H. S. Xu *et al.*, Phys. Rev. Lett **85**, 716 (2000).
[16] J. D. Frankland *et al.*, Nucl. Phys. A **689**, 940 (2001).
[17] S. Mallik, G. Chaudhuri, and S. Das Gupta, arXiv:1503.04929 [nucl-th].
[18] G. Chaudhuri, S. Das Gupta, and M. Sutton, Phys. Rev. B **74**, 174106 (2006).
[19] G. Chaudhuri and S. Das Gupta, Phys. Rev. C **80**, 044609 (2009).
[20] J. P. Bondorf, A. S. Botvina, A. S. Iljinv, I. N. Mishustin, and K. Sneppen, Phys. Rep **257**, 133 (1995).
[21] A. Botvina, G. Chaudhuri, S. Das Gupta, and I. Mishustin, Phys. Lett. B **668**, 414 (2008).
[22] S. R. Souza *et al.*, Nucl. Phys. A **571**, 159 (1994).
[23] S. Leray *et al.*, Nucl. Phys. A **531**, 177 (1991).
[24] J. Aichelin and G. F. Bertsch, Phys. Rev. C **31**, 1730 (1985).